Scholar Publishing Group
Frontiers in Ocean Engineering
https://doi.org/10.38007/FOE.2022.030303
ISSN 2790-2706 Vol. 3, Issue 3: 21-29

Hydrodynamics of Double Tanks in Narrow Environment in Ocean Engineering Based on Boundary Finite Element Method

Garg Sahil*

Monash Univ Malaysia, Selangor Darul Ehsan 47500, Malaysia

**corresponding author*

Keywords: Boundary Finite Element Method, Ocean Engineering, Narrow Environment, Double Tank Hydrodynamics

Abstract: Due to the great application value of super-large floating body in ocean engineering, there have been many studies on it in the past 20 years. In fact, a super-large floating body is composed of many small floating bodies, and there are slits between them. The hydrodynamic interaction between the small floating bodies is a complex hydrodynamic interference problem. For the hydrodynamic analysis research of super-large floating bodies composed of many small floating bodies, traditional numerical methods have encountered certain difficulties. In this paper, the purpose of this paper is to study the hydrodynamics of double tanks in the narrow gap environment of marine engineering based on the boundary finite element method. This paper uses the numerical simulation method. Based on the successful simulation of a single cage, the double cage composed of two single cage The hydrodynamic characteristics under the action of water flow are studied, which will lay a strong foundation for the development of deepwater multi-body combined cage research. Based on the basic theory of fluid mechanics, the hydrodynamic resistance of deep-water vessels is estimated. The complex and changeable model is replaced by an ideal model, and the resistance of the cage is divided into three parts: rod , ring and net, and the resistance of the rest is ignored. A simple formula is obtained by mathematical fitting and the error is estimated within the allowable range. Follow the steps for a scientific assessment of cage hydrodynamics using accepted formulas .

1. Introduction

In order to achieve specific functional requirements such as mining, transportation and unloading of marine resources, super-large marine structures are generally composed of several modules, such as large fleets and marine platforms. The ships and platforms are not simply connected seamlessly.

There are generally small slits between these structures that are much smaller than their own characteristic scales. Relevant studies have proved that under the action of certain cycles of waves, the water in the slits between the floating structures will have a relatively large amplitude. The motion corresponds, that is, the resonance phenomenon occurs. This dramatically increases the loading of the water on these structures, inducing larger wave climbs. It directly affects the normal safe operation of the structure. Scholars from all over the world have fully studied the hydrodynamic effects of narrow seams on marine structures, but most of them are limited to the case where the draught of the floating bodies is the same and the shape of the box is regular. Due to the difference in load, the draught of the floating body will also be different, and the floating body is not a completely regular rectangular box. Therefore, it is of great theoretical and practical significance to study the draught on the hydrodynamic properties in the narrow gap between floating bodies [1-2] .

In the research on the hydrodynamics of double tanks in the narrow environment of marine engineering based on the boundary finite element method , many scholars have studied it and achieved good results. For example : Najafi S When the size of the gap between the floating bodies is much smaller than its When the resistance is encountered, the asymptotic correlation method is used to solve the influence of the gap on the hydrodynamic effect of the floating body [3]. Both the space near the end of the slit and the inner space far from the slit of Ghafari HR adopt the corresponding expansion form; the external remote field adopts the eigenfunction expansion method. Outside the far-field, the input to the pulsed source is determined, and the unknowns in the expansion have corresponding asymptotic determinations between domains [4].

In this paper, based on the potential flow theory, the advanced high-order boundary element method is used to construct a completely non-numerical numerical model of lumen, and the influence of current on the water resonance phenomenon between the two-slot slits is studied. The normal wave is generated by the source wave, and the free surface has completely inhomogeneous kinematics and dynamic boundary conditions. There are damping layers on both sides of the calculation surface to absorb the outgoing wave and avoid the influence of the reflected wave. Artificial damping was placed on the free water surface between the slits to approximate the viscosity dissipation due to eddy shedding and water flow separation. The artificial damping coefficient of the fluid between the slits in the numerical model is determined. In addition, experimental and numerical methods were used to study the effect of floating body design on the resonance characteristics (resonance frequency and resonant wave height) of the narrow slit water body, the power-law effect of the power-law slit on the water viscosity, and the wave height of the groove and the return wave side and wave height law of influence. At the same time, the influence of wave propagation direction is also studied in this paper.

2. Research on the Hydrodynamics of the Double Tank in the Narrow Environment of Marine Engineering Based on the Boundary Finite Element Method

2.1. Finite Element Method and Theory

When checking the strength of an engineering project with a complex shape and structure, it is very complicated, cumbersome and even impossible to deduce its analytical formula. The finite element method "fills" a complex research object with a large number of simple elements through the idea of discrete approximation, and replaces the entire complex research object by analyzing a limited number of elements. The numerical solution obtained by the finite element is an approximation of the complex differential equation of the original problem, so its accuracy is affected by the performance of the grid element [5-6] .

The finite element inverse method used in this paper is a combination of finite element theory

and inverse problem. This method reverses the traditional finite element process and is based on the finite element mathematical model. Therefore, finite element modeling will be introduced here basic process. The first step of finite element analysis is to establish an initial model according to the structure, material and boundary conditions of the research object. Then select different element types according to the needs of the problem. The essence of the element type is the difference between the interpolation functions. The more the number of nodes, the better the approximation effect. The quadratic interpolation function is a parabola, which can describe the curve compared to the linear isoparametric element boundary. The third step is to divide the mesh to discretize the research object, and use a large number of elements to express the research object. These two steps have a great influence on the results of the finite element. The finite element usually takes displacement as the basic variable. The principle of virtual displacement or the principle of minimum potential energy is used to establish a balance equation between the assembled overall stiffness matrix and the external force of the structure. The key to the solution process is to ensure the convergence of the numerical solution and the convergence of the solution. It is related to the approximation method of finite element theory, and is also related to the division technology, shape and performance of the mesh. Generally speaking, the smaller the mesh size of the finite element, the higher the performance of the element, the more accurate the analysis results and the greater the computational cost [7-8].

2.2. Influence of Draft on the Resonance Characteristics of the Water Body Between the Narrow Slits of the Double Tank

In the case of different wave propagation directions, the resonance characteristics between the slits of the boxes with different draught combinations also have obvious differences. In the two-dimensional case, no matter which direction the wave propagates, the resonance frequency of the water body between the slits remains unchanged. When d1=(5/12)B remains unchanged and d2 gradually increases to (5/12)B, the resonant wave height and fluid viscosity effect of the water body in the narrow slit when the wave propagates to the left are greater than those when the wave propagates to the right. When d2 continues to increase from (5/12)B, when the wave propagates to the left, the resonant wave height and fluid viscosity effect of the water body in the narrow slit are smaller than those when the wave propagates to the right; when the draught of the two boxes is the same, The direction of wave propagation has no effect on it. By comparison with the case of the same draught as the box, it can be found that no matter which direction the wave propagates, when the draughts of the two boxes are relatively large, the resonant wave height of the water body in the narrow gap is the largest [9-10]. At the same time, when the wave propagation direction is from a box with a smaller draught to a box with a larger draught, the resonant wave height of the water body in the narrow slot of the box is larger than that in the opposite direction of wave propagation. When the draught of the tank on the wave-facing side takes a relatively small value and the draught of the tank on the back-wave side takes a relatively large value, compared with other draught combinations, the fluid viscous effect between the slits is the strongest; When the depth takes a relatively large value and the draught depth of the tank on the back wave side takes a relatively small value, compared with other draft combinations, the fluid viscosity effect between the slits is the weakest [11-12].

2.3. Algorithm Selection

The boundary conditions can be written in the following form:

$$\frac{DX(x,z)}{Dt} = \nabla\phi \tag{1}$$

$$\frac{D\phi}{Dt} = -g\eta + \frac{1}{2}|\nabla\phi|^2 \tag{2}$$

Where: X(x, z) is the instantaneous position of the fluid particle on the free water surface, η representing the height of the wave surface, and g is the acceleration of gravity. The sum of the right-hand terms $\mu_1(x)\phi$ of $2\mu(gk)^{0.5}\phi$ the two equations $k\mu_2^2$ is the damping term, which is used to approximate the viscous dissipation caused by flow separation and vortex shedding in the narrow slit $\mu_1(x)(X - X_0)$. , which is used to simulate the damping term in the upstream and downstream regions of the free surface computational domain to absorb reflected waves and outflow waves [13-14] .

3. Research and Design Experiment of Double-Tank Hydrodynamics Based on Boundary Finite Element Method in Narrow Gap Environment In Marine Engineering

3.1. Introduction of Experimental Equipment and Instruments

The wave machine used in this experiment is a one-way push-plate wave machine, which is located at the front end of the wave flow tank. This one-way push-plate wave machine has high wave-making accuracy and can produce stable regular waves. Several layers of wave damping sills are set at the end of the wave flow tank, so as to reduce the influence of wave reflection on the experiment as much as possible, and ensure the stability and repeatability of the created waves. During the experiment, the LG-70 wave height meter was used to collect the experimental data. This type of wave height meter has high precision (10-5 m) and small error [15] .

3.2. Data Processing and Collection

Experimental wave:

In order to improve the accuracy of the experiment as much as possible, it is necessary to make waves before placing the experimental model, that is, to pre-assemble the wave elements of each experimental group and working condition. It can be divided into the following steps: first, calibrate and preheat multiple wave height meters, put them in order and fix them in the wave flow tank where the box will be arranged, and then read a preset wave height into the wave generator. After the waves are produced, the actual incident wave height and period are measured by these wave height meters, and compared with the wave elements required in the experimental conditions. If the difference is large, the input wave height and period are adjusted accordingly, and the cycle begins Until it is basically consistent with the required wave elements, stop when the accuracy required by the experiment is met, and save the final wave-making file to complete the wave creation. The above steps can be repeated to complete all experimental conditions [16-17].

Data collection and processing:

After the experimental wave is completed, the box model can be arranged and fixed, the wave height meter can be installed and preheated. After the preheating is completed, the still water surface can be zeroed, and the appropriate wave-making file can be selected according to the relevant experimental group. To create a wave, data can be collected after the wave surface is stable. In the experiment, the sampling interval of the data acquisition system is 0.01 seconds, and the data acquisition length is 4096 seconds.

Under the same working conditions, at least two repeated tests must be carried out. After the data collection of each test is completed, the next test should be carried out after the still water surface is calm again, and the wave height meter is reset to zero again. Under the same working condition, the measurement results of the second experiment must meet the accuracy requirements, otherwise the experiment under this working condition will be continued. Repeat the above steps until all the wave condition experiments are completed [18] .

4. Experimental Analysis of Double Tank Hydrodynamics Based on Boundary Finite Element Method in Narrow Gap Environment in Marine Engineering

4.1. Resonant Frequency and Resonant Wave Height

When the draught depths of the two boxes are exactly the same, in order to study the influence of draught on the resonance characteristics of the water body between narrow slits, three sets of experiments are carried out in this paper, namely: ① d1=0.20m, d2=0.20m. ② d1=0.25m, d2=0.25m. ③d1=0.30m, d2=0.30m After the damping coefficient in the numerical model is determined from the experimental data, the wave height changes between the slits under the three groups of draft conditions are shown in Table 1 .

Table 1. Wave height variation between narrow seams in three drafts

	D1=D2=(4/12)B	D1=D2=(5/12)B	D1=D2=(6/12)B
Resonant frequency	3.4	2.96	2.57
Resonance wave height	2.20	2.59	2.72

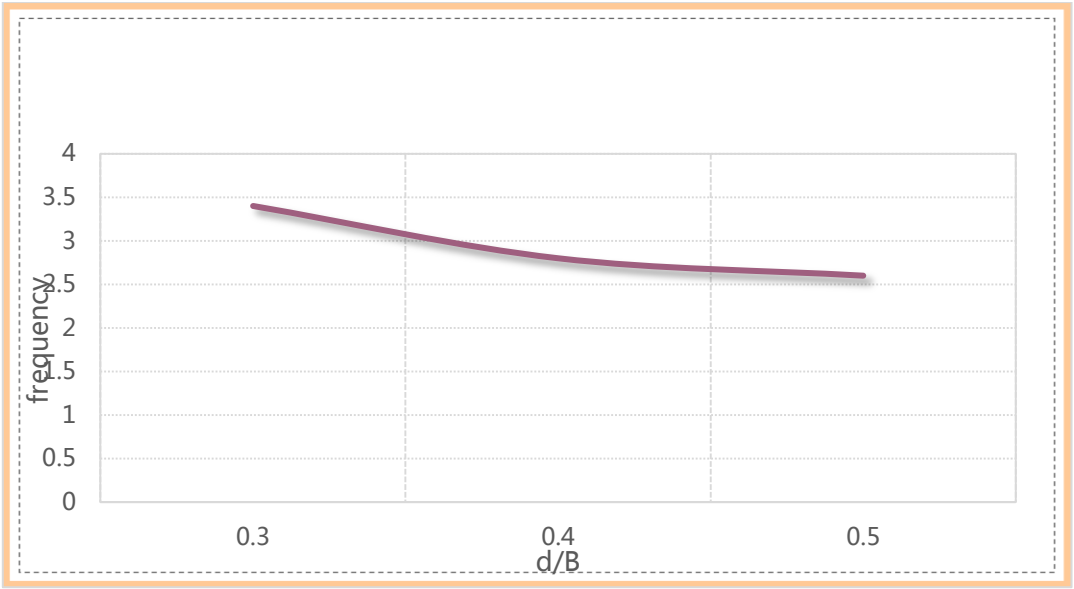

Figure 1. The change law of narrow-seam resonance frequency with draft depth

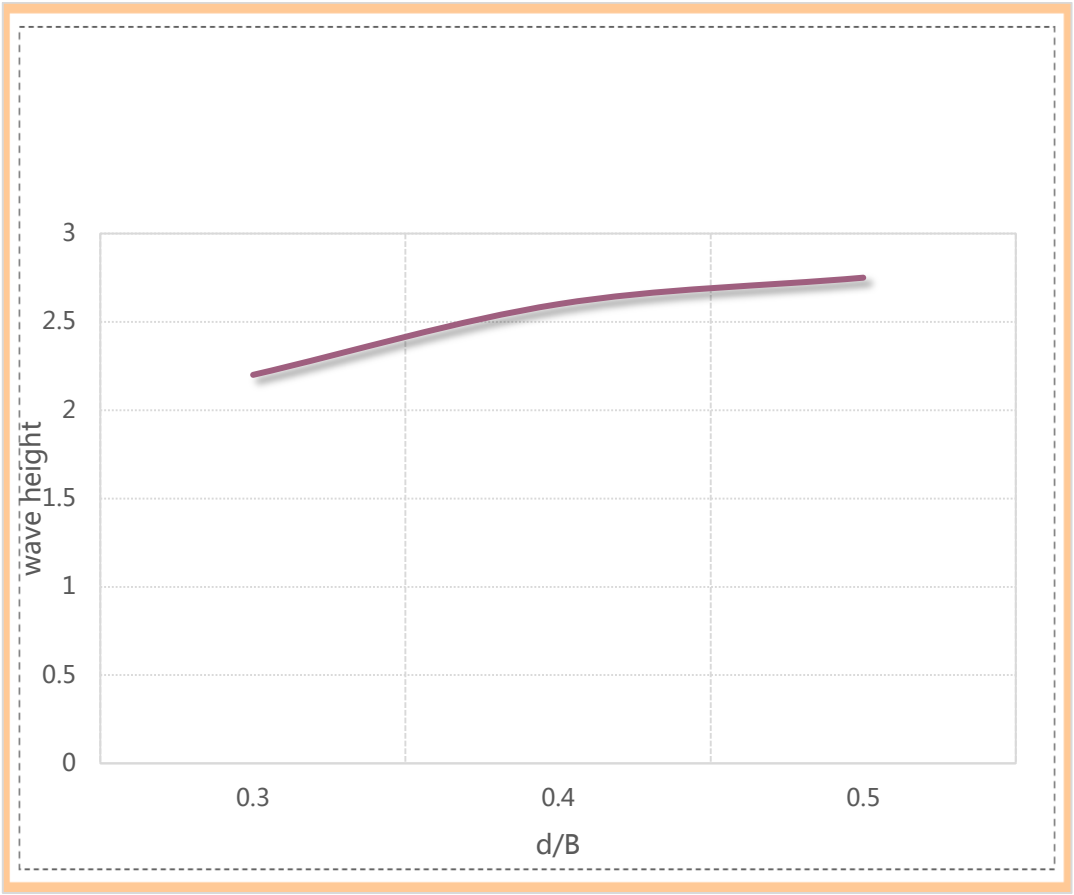

Figure 2. Change law of resonance wave height with draft depth

Figures 1 and 2 show the resonant frequency kh between the slits and the dimensionless resonant wave height Hg/H0 with the dimensionless draught d/B of the two boxes at the same draught. The variation law approximates the fitting curve, and it can be seen that with the continuous increase of the draught, the resonance frequency of the water body between the narrow slits continues to decrease, while the resonance wave height gradually increases. This is because the resonance frequency is mainly related to the quality of the resonant water body between the slits. With the increase of the draft, the mass of the resonance water body between the slits increases, resulting in a decrease in the resonance frequency and an increase in the resonance wave height.

4.2. Fluid Viscosity Effect between Slits

This paper , because the mechanical energy dissipation in the fluid is ignored, the resonance wave height between the slits obtained by this model is often larger than the actual value. The numerical model proposed in this paper μ_2 simulates the viscous dissipation caused by fluid vortex shedding and flow separation by setting artificial damping with a damping coefficient of 1 on the free water surface between the slits. The damping coefficient μ_2 can approximately characterize the fluid viscous effect between slits. By comparing the numerical model and experimental data, the damping coefficients of these three groups of experiments with the same draft can be determined. The data are shown in Table 2.

Table 2. Damping coefficient of the same draft experiment groups

	0.3	0.4	0.5
Damped coefficient	0.0472	0.045	0.043

Figure 3. Change of viscosity coefficient between narrow joints with draft depth

Figure 3 shows the variation curve of the viscosity coefficient of the free water surface between the narrow slits of the double tanks μ_2 with the draft depth of the tank. The viscosity coefficient between slits decreases slightly, and the effect of fluid viscosity between slits decreases, but the effect is not very significant.

5. Conclusion

This paper is based on the potential flow theory, and the fluid viscosity effect between the slits is slightly weakened. With the increase of the incident wave number, the wave height on the front side of the box shows a fluctuating trend, and there is an obvious trend of decreasing first and then increasing near the resonance frequency, while the wave height on the back side of the box gradually decreases, and at the resonance frequency There is a significant reduction around the frequency. In the case of three different drift angles, the fluid between the slits also appeared resonance phenomenon. The experimental wave height at the front end of the system fluctuates up and down, while the experimental wave height value at the back end of the system decreases

continuously with the increase of the incident wave number. At the narrow slit, with the increase of the outer drift angle, the range of the resonance interval measured by the experiment is expanded; for the front end of the system, in the resonance region, the larger the outer drift angle of the box is, the greater the measurement point will be. The smaller the experimental wave height value is; at the rear end of the system, the larger the external drift angle of the box, the larger the experimental wave height value at the measuring point . The increasing trend of water resonance wave height between narrow fractures slows down, and the fluid viscosity effect between narrow fractures increases. Both head-side wave heights and back-side wave heights have local sudden changes near the resonance frequency. The head-side wave heights first become smaller and then larger, and the back-side wave heights decrease sharply. Through the comparison with the case of the same draft depth of the tank, it can be found that the resonance frequency of the water body between the narrow slits of two tanks with different drafts is greater than the case where the drafts of the two tanks are both larger, and is smaller than that of the two tanks. The case where the draft depth of each box is small.

Funding

This article is not supported by any foundation.

Data Availability

Data sharing is not applicable to this article as no new data were created or analysed in this study.

Conflict of Interest

The author states that this article has no conflict of interest.

References

[1] Wang P , Zhao M , Du X , et al. A finite element solution of earthquake-induced hydrodynamic forces and wave forces on multiple circular cylinders. Ocean Engineering, 2019, 189(Oct.1):106336.1-106336.11. https://doi.org/10.1016/j.oceaneng.2019.106336

[2] Mei T L , Zhang T , Candries M , et al. Comparative study on ship motions in waves based on two time domain boundary element methods. Engineering analysis with boundary elements, 2020, 111(Feb.):9-21. https://doi.org/10.1016/j.enganabound.2019.10.013

[3] Najafi S , Abbaspoor M . Numerical investigation of flow pattern and hydrodynamic forces of submerged marine propellers using unsteady boundary element method:. Proceedings of the Institution of Mechanical Engineers, Part M: Journal of Engineering for the Maritime Environment, 2019, 233(1):67-79. https://doi.org/10.1177/1475090217717174

[4] Ghafari H R , Ketabdari M J , Ghassemi H , et al. Numerical study on the hydrodynamic interaction between two floating platforms in Caspian Sea environmental conditions. Ocean Engineering, 2019, 188(Sep.15):106273.1-106273.11. https://doi.org/10.1016/j.oceaneng.2019.106273

[5] Wan R , Jia M , Guan Q , et al. Hydrodynamic performance of a newly-designed Antarctic krill trawl using numerical simulation and physical modeling methods. Ocean Engineering, 2019, 179(MAY 1):173-179. https://doi.org/10.1016/j.oceaneng.2019.03.022

[6] Angelou M , Spyrou K J . Modeling of transient hydrodynamic lifting forces of sailing yachts and study of their effect on maneuvering in waves. Ocean Engineering, 2019,

173(FEB.1):531-547. https://doi.org/10.1016/j.oceaneng.2019.01.021

[7] Huang H , Zou M S , Jiang L W . Study on the integrated calculation method of fluid-structure interaction vibration, acoustic radiation, and propagation from an elastic spherical shell in ocean acoustic environments. Ocean Engineering, 2019, 177(APR.1):29-39. https://doi.org/10.1016/j.oceaneng.2019.02.032

[8] Tafazzoli S , Shafaghat R , Alamian R . Optimization study of a catenary mooring system for a spar floating wind turbine based on its hydrodynamic responses:. Proceedings of the Institution of Mechanical Engineers, Part M: Journal of Engineering for the Maritime Environment, 2021, 235(2):657-674. https://doi.org/10.1177/1475090220917812

[9] Firouz-Abadi R D , Panah M . Development of an aeroelastic model based on system identification using boundary elements method. Aircraft Engineering and Aerospace Technology, 2022, 94(3):360-371. https://doi.org/10.1108/AEAT-01-2021-0025

[10] Duan J S , Rach R , Wazwaz A M . Simulation of the eigenvalue problem for tapered rotating beams by the modified decomposition method. International Journal for Computational Methods in Engineering Science and Mechanics, 2022, 23(1):20-28. https://doi.org/10.1080/15502287.2021.1904461

[11] Zorya I V , Poletaev G M , Rakitin R Y . Influence of Carbon and Oxygen Impurities on the Migration Rate of 110 Tilt Boundaries in Austenite. Steel in Translation, 2022, 52(2):151-156. https://doi.org/10.3103/S0967091222020267

[12] Belykh V N . Unsaturated Algorithms for the Numerical Solution of Elliptic Boundary Value Problems in Smooth Axisymmetric Domains. Siberian Advances in Mathematics, 2022, 32(3):157-185. https://doi.org/10.1134/S1055134422030014

[13] Zhang L , Wang C , Sun J , et al. Study on the hydrodynamic aggregation of parallel self-propelled flexible plates based on a loosely coupled partitioned algorithm. Ocean Engineering, 2021, 223(2):108703. https://doi.org/10.1016/j.oceaneng.2021.108703

[14] Kim S J , Kim M H , Koo W . Nonlinear hydrodynamics of freely floating symmetric bodies in waves by three-dimensional fully nonlinear potential-flow numerical wave tank. Applied Ocean Research, 2021, 113(1-2):102727. https://doi.org/10.1016/j.apor.2021.102727

[15] Biswas S , Schwen D , Hales J D . Development of a finite element based strain periodicity implementation method. Finite Elements in Analysis and Design, 2020, 179(12):103436. https://doi.org/10.1016/j.finel.2020.103436

[16] Liang H , He S , Liu W . Dynamic simulation of rockslide-debris flow based on an elastic–plastic framework using the SPH method. Bulletin of Engineering Geology and the Environment, 2020, 79(1):451-465. https://doi.org/10.1007/s10064-019-01537-8

[17] Stewart S A , Moslemi-Tabrizi S , Smy T J , et al. Scattering Field Solutions of Metasurfaces based on the Boundary Element Method (BEM) for Interconnected Regions in 2D. IEEE Transactions on Antennas and Propagation, 2019, PP(99):1-1. https://doi.org/10.1109/TAP.2019.2935131

[18] Jong-Shyong W U , Wang J R , Chen D W , et al. Study On Dynamic Stability And Free Vibrations Of Multi-Span Fluid-Conveying Pipes In Water With Various End Conditions. International Journal of Applied Engineering Research & Development, 2019, 9(1):29-63.